

Colored-noise-induced chaotic array synchronization

M. N. Lorenzo* and V. Pérez-Muñozuri†

Group of Nonlinear Physics, Faculty of Physics, University of Santiago de Compostela, 15706 Santiago de Compostela, Spain
(Received 14 October 1998; revised manuscript received 25 March 1999)

The effect of a time-correlated Gaussian noise on one-dimensional arrays consisting of diffusively coupled chaotic cells is analyzed. A resonance effect between the time scale of the chaotic attractor and the colored Gaussian noise has been found. As well, depending on the number of cells, coupling, and noise strength, an improvement of the synchronization or a poor synchronization between cells within the array can occur for some values of the time correlation. These nonlinear cooperative effects are studied in terms of a linear stability analysis around the uniform synchronized behavior. [S1063-651X(99)02109-1]

PACS number(s): 05.45.-a, 05.40.-a

I. INTRODUCTION

The behavior of nonlinear dynamical systems in the presence of small perturbations and noise has been the subject of numerous and extensive studies. In particular, the dynamics of chaotic systems depends sensitively on tiny perturbations of the initial values. Then, perturbations can be added in a controlled (control theory [1,2]) as well as uncontrolled way as is the case in the presence of noise (noise-induced chaos [3,4], stochastic resonance [5–8]).

Noise can play a constructive role in the detection of weak periodic signals via a mechanism known as *stochastic resonance*. In essence, stochastic resonance is a further remarkable nonlinear cooperative phenomenon, in which the signal-to-noise ratio of a periodically modulated system can be amplified by the addition of external noise. Nonlinear cooperative effects between periodic and random perturbations may imply that incoherent noise leads to a coherent output signal (e.g., in ring lasers [9]). Now, this effect has been reported in a wide variety of physical systems [10–13], and biology [14–16].

More recently, the presence of noise in ensembles of chaotic systems has been studied as a function of the coupling strength among systems. For coupled chaotic systems, white Gaussian noise can be used to control spatiotemporal chaos [17–20]. In particular, the term *array-enhanced stochastic resonance* was recently introduced by Lindner *et al.* [21] to describe spatiotemporal stochastic resonance in a numerical model of coupled, bistable oscillators. They derived scaling laws for the optimum noise intensities and coupling strengths resulting in an optimization of the signal-to-noise ratio as a function of the number of oscillators. As a clear example of these studies, chaotic behavior in spatially extended systems, especially in biology and physiology [22–24], might be amenable to control, as it is the case in low-dimensional chaotic systems. This control eventually leads to the formation of regions whose chaotic cells are synchronized to each other, giving rise to spatial patterns or clusters that interact with each other with time.

On the other hand, the behavior of uncoupled chaotic systems under the influence of external noise has been the subject of recent work [25–32]. The main idea behind this research is that uncoupled chaotic systems cannot be synchronized by means of an identical noise signal (Gaussian noise of zero mean), except for a noise with some non-zero bias.

In this paper, the role of a time-correlated Gaussian noise in diffusively coupled chaotic cells is analyzed. In recent times, white noise has been replaced by colored noise in a variety of contexts. The noise color significantly enriches the fluctuation dynamics, particularly where the characteristic correlation time of the noise is not small compared to the time scale of the system [33,34]. Laser noise problems [35] and first passage problems [36] are some examples that have been shown to necessitate the use of colored noise instead of white noise. On the other hand, for nonlinear dynamical systems without periodic external force parametrically perturbed with colored noise, a nonmonotonic behavior of the coherence in the system response was observed as a function of the noise correlation time, while no coherence enhancement was measured when the noise amplitude was varied [37,38]. Our aim in this paper is to investigate the nonlinear cooperative effects of noise strength, correlation time, and length scales to control spatiotemporal chaos in coupled arrays of chaotic cells.

II. MODEL

In our simulations, a one-dimensional array, consisting of diffusively coupled chaotic cells of the Lorenz type, was used,

$$\begin{aligned} \dot{x}_j &= \alpha(y_j - x_j), \\ \dot{y}_j &= [R + \xi_j(t)]x_j - y_j - x_j z_j + D(y_{j+1} + y_{j-1} - 2y_j), \\ \dot{z}_j &= x_j y_j - b z_j, \end{aligned} \quad (1)$$

with α , R , and b positive parameters [39]. Usual parameter values are $\alpha = 10$, $b = \frac{8}{3}$, and $R = 28$. By keeping α and b constants while varying R , it is possible to simplify the linear stability analysis [40] which will be useful later in the discussion. The origin is stable for $R < 1$. At $R = 1$ the origin

*Electronic address: nieves@fmnmeteo.usc.es

†Electronic address: vicente@fmnmeteo.usc.es; http://fmnmeteo.usc.es

loses stability by a supercritical pitchfork bifurcation, and a symmetric pair of attracting points is born. At $R_{\text{cr}}=24.74$ the fixed points lose stability by absorbing an unstable limit cycle in a subcritical Hopf bifurcation and the nonlinear set becomes a strange attractor.

In Eq. (1), D accounts for the coupling diffusion coefficient between cells, j runs from 1 to N (number of cells in the array), and $\xi(t)$ is a colored Gaussian noise of zero mean whose dynamics is given by

$$\dot{\xi} = -\tau^{-1} \xi + \tau^{-1} \xi_w(t). \quad (2)$$

The Ornstein-Uhlenbeck stochastic process $\xi(t)$ [41] is driven by the white Gaussian noise $\xi_w(t)$ with $\langle \xi_w(t) \rangle = 0$ and $\langle \xi_w(t) \xi_w(t') \rangle = 2A \delta(t-t')$. The correlation function of $\xi(t)$ is an exponential function given by

$$\langle \xi(t) \xi(t') \rangle = \frac{A}{\tau} \exp\left(-\frac{|t-t'|}{\tau}\right), \quad (3)$$

where τ is the correlation time, A is the noise amplitude, and $\sigma = \sqrt{A/\tau}$ is the noise dispersion. In the limit $\tau \rightarrow 0$ the white-noise limit $\xi_w(t)$ is recovered.

We emphasize here two cases; incoherent or *local noise*, where the noise is uncorrelated from site to site, and *global noise*, where the noise is identical at each site [42]. In this work, noise is added to the control parameter R resulting in a multiplicative contribution to the evolution equations. Although we will show the existence of optimal values of coupling strength and color noise that lead to an improvement or to a worsening of the synchronization between chaotic cells, we expect that this behavior can also be found when noise is added to the system in a different way.

Equation (1) was numerically integrated using an explicit Euler method with a time step of 10^{-4} . Free ends (zero flux) and periodic boundary conditions were considered. The exponentially correlated noise $\xi_j(t)$ was numerically calculated at each site j by an integral algorithm suggested by Fox *et al.* [43] instead of solving Eq. (2). Random initial conditions for all variables were given to each cell in the array.

In order to characterize the *degree* of synchronization between cells of the array, we introduce the following time-averaged quantity:

$$K = \lim_{T \rightarrow \infty} \frac{1}{T} \sum_{t=1}^T \left(\frac{1}{N-1} \sum_{j=2}^N \left\| \vec{u}_j^t - \vec{u}_{j-1}^t \right\| \right), \quad (4)$$

with $\vec{u} = (x, y, z)$ and $\|\cdot\|$ represents the Euclidean distance. This function is positive defined and it is equal to zero when all the cells in the array are globally synchronized. As K may serve as a measure of the array complexity, in this context it can be related to the Kolmogorov-Sinai entropy [44]. Numerical simulations were run until K varied less than 5%.

In the same context, in order to analyze the behavior of the array under the presence of noise, it is possible to calculate the transverse Lyapunov exponents corresponding to the transverse perturbation to the synchronized manifold. Nevertheless, while this spectrum can be easily calculated for an array with periodic boundary conditions forced with correlated colored noise, this is not the case for an array with free ends or an array consisting of cells forced with local or un-

correlated noise. In the Appendix, the linear stability analysis performed to calculate the transverse Lyapunov spectrum is depicted.

III. RESULTS

The main effect of a colored Gaussian noise on an array of diffusively coupled chaotic Lorenz systems is shown in Figs. 1 and 2. Results are shown separately for local (Fig. 1) and global (Fig. 2) noise, as a function of the time correlation τ , number of cells in the array, and coupling strength. For low values of the diffusion (upper rows in Figs. 1 and 2), independently of the specific values, the dependence of K on τ is equivalent for all the arrays considered; as τ is increased, a maximum of K is observed at $\tau = \tau_R$, and for $\tau \rightarrow \infty$, K tends to K_0 (i.e., the value of K obtained for the same array without considering the presence of noise). The only effect of the global or space-correlated noise in comparison to the local noise is to attenuate the curve near the maximum at $\tau = \tau_R$. Note as well that for $N=20$ and $N=100$, the maximum value of K is approximately the same but greater than that measured for $N=4$. Since K measures the *degree* of synchronization between cells, and $K - K_0$ is greater than zero, the effect of noise for low values of D is to deteriorate the synchronization, at least within the range of values of τ near τ_R .

On the other hand, for high values of the coupling strength (lower rows in Figs. 1 and 2), the effect of the colored Gaussian noise on arrays consisting of chaotic cells is the opposite to the one described above. That is, as τ is increased K diminishes, later increases near $\tau = \tau_R$, again it decreases for $\tau > \tau_R$, and finally attains a constant value equal to K_0 . As N increases, the maximum value of K also increases, leading to a global displacement of the curve towards positive values (see, for example, the figure for $N = 100$), although τ_R was not found to depend on N . As well, as described above, the main effect of the correlated noise is to damp and smooth the curve near the value of τ_R .

In the same way, the two limits $\tau \rightarrow 0$ and $\tau \rightarrow \infty$ are equivalent for both cases; local and global noise. When $\tau \rightarrow 0$, the white Gaussian noise limit is recovered and cells within the array do not become synchronized to each other independently of the variance of the noise [32]. Only the coupling diffusion term allows to some extent the synchronization among the different units in the array. Similarly, when $\tau \rightarrow \infty$ the term $\xi(t)$ in Eqs. (1) behaves as a constant value different for each cell. Noise affects the strange attractor dynamics that becomes asymmetric, while no synchronization is observed between cells within the array. For high enough noise amplitude, the main effect will be a biased signal that will induce a regularization in the system. This effect is analogous to that of some chaos suppression methods that can achieve this result through perturbations in the system variables [45].

The effect of the periodic boundary conditions on arrays of diffusively coupled chaotic cells forced with colored Gaussian noise is analyzed in terms of the highest Lyapunov exponent $\lambda(q)$ calculated from Eq. (A3). Figure 3 shows a three-dimensional plot of the highest transverse Lyapunov exponent $\lambda(q, \tau)$ as a function of $\log_{10} \tau$ and the reduced wave number $q = k/N$ for $D = 0.5$. Note that for any value of

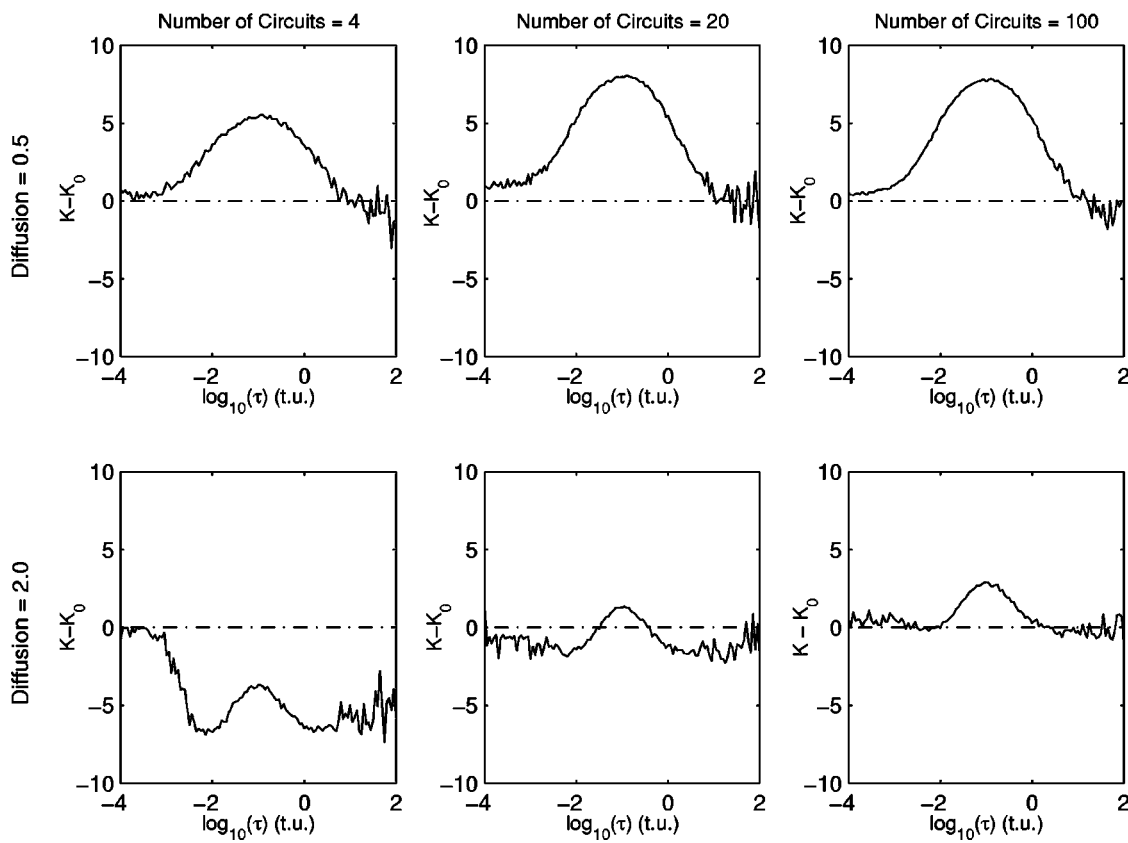


FIG. 1. Dependence of $K - K_0$ as a function of $\log_{10}\tau$ for different values of the coupling diffusion coefficient D and number of chaotic cells N within the array. Local or uncorrelated noise is herewith considered; $\xi_i(t) \neq \xi_j(t) \forall i, j = 1, \dots, N$. Parameter values: $\sigma = 3$ and free ends were considered in the integration of Eq. (1).

$\log_{10}\tau$, $\lambda(q)$ is symmetric with respect to the line $q = 1/2$ as described in the Appendix. On the other hand, for any value of q , the behavior of $\lambda(\tau)$ is equivalent to the results shown in Fig. 2 obtained with Eq. (4); i.e., a maximum of $\lambda(\tau)$ occurs for some τ_R . The function $\lambda(q, \tau)$ crosses the zero line (shown as a plane in Fig. 3) to become negative for some values q_c and τ_c . The wave number q_c signals the instability of the ring, and the lowest possible value of N for which the $k=N q_c$ condition can be fulfilled is for $k=1$. As k is an integer variable, this implies that the critical size of the ring N_c is defined by the lowest N for which $N_c q_c \geq 1$ for some time correlation τ_c . Thus, for some discrete values of q_c (see Table I), there exists a minimum value τ_c for which $\lambda(q, \tau)$ is negative, and the dynamics of the array bifurcates from a nonsynchronized state to a synchronized one. As described above for $K(\tau)$, at the limit $\tau \rightarrow \infty$, $\lambda(q, \tau) \rightarrow \lambda(q, \tau \rightarrow 0)$.

Figure 4 illustrates the behavior of $K - K_0$ as a function of the noise dispersion σ and time correlation τ for a given length of the array and coupling diffusion. Note that independently of the value of σ , the curve shape is kept unchanged like the ones described above, with a single peak that develops around $\tau = \tau_R$ (see the profiles of $K - K_0$ obtained for different values of σ as a function of τ). The role of σ is to increase the maximum value of $K - K_0$ and to make wider the peak around τ_R . Then, no stochastic resonance effect was found as the noise amplitude is changed [37,38]. As σ increases, larger values of τ are needed in order for K to relax towards K_0 .

By varying the coupling diffusion coefficient between chaotic cells, the value of τ that corresponds to the maximum of K , τ_R , decreases with increasing D for a constant noise dispersion as is shown in Fig. 5. For $D \rightarrow 0$, no improvement or worsening of the synchronization between cells was found for any value of τ (K remains approximately constant), in agreement with Refs. [25–32]. Besides, the maximum value of K was found to linearly decrease as D increases. The same behavior of $\tau_R(D)$ for a small number of circuits in the array shown in Fig. 5 was found for greater values of N .

Near the onset of resonance, τ_R , the dynamics of the array could be simplified to that of a chain of linearly coupled oscillators, forced periodically with a frequency equal to τ_R^{-1} , whose dynamics is described in terms of a plane wave solution. The wave frequency ω and coupling diffusion coefficient are related through the wave dispersion equation, $\omega \propto \sqrt{D}/\lambda$, with λ the wavelength. For small size arrays, it can be considered that λ is fixed by the boundary conditions and then it remains constant. This is in agreement with our simulations where we have found that $\tau_R \propto 1/\sqrt{D}$ independently of the length of the array. Obviously, the explanation above is a simplification of the problem, since the chaotic dynamics cannot be mapped in a simple way to that of an oscillator. Nevertheless, our aim is to stress the similarity between the classical frequency locking problem that occurs in a chain of oscillators forced periodically and the behavior of K for $\tau \approx \tau_R$. Here, the locking does not occur for a single value of the frequency, but for a range of frequencies that gives rise to a wide behavior of K as a function

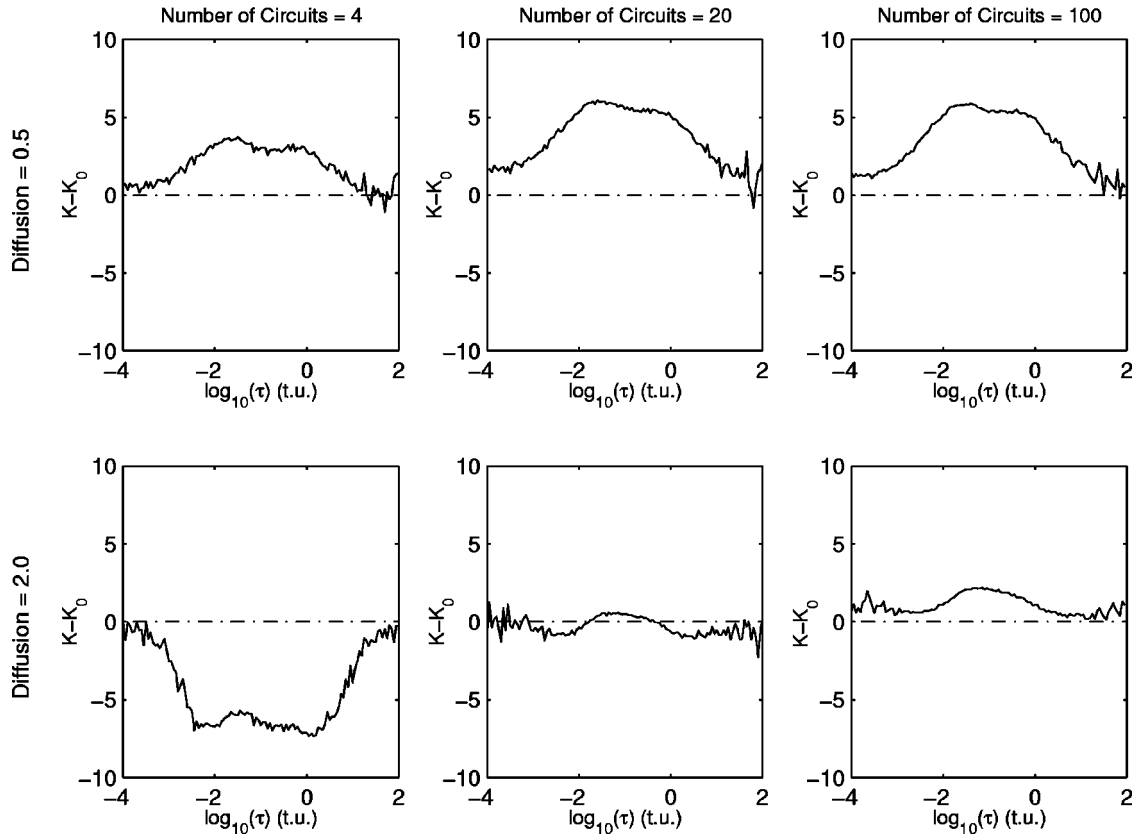


FIG. 2. Dependence of $K - K_0$ as a function of $\log_{10}\tau$ for different values of the coupling diffusion coefficient D and number of chaotic cells N within the array. Global or space-correlated noise is herewith considered; $\xi_i(t) = \xi_j(t) \forall i, j = 1, \dots, N$. Parameter values: $\sigma = 3$ and free ends were considered in the integration of Eq. (1).

of τ near the onset of resonance.

The influence of the bifurcation parameter R on the previous results is shown in Fig. 6. Since noise $\xi(t)$ is added to R in Eq. (1), the selected value of R should influence the

observed dynamics the closer this value is taken to the bifurcation point at $R = R_{\text{cr}}$. Thus, from the three-dimensional plot of $K - K_0$ shown in Fig. 6(a), it is possible to note that as R is increased, the function $K(\tau)$ shows a global displace-

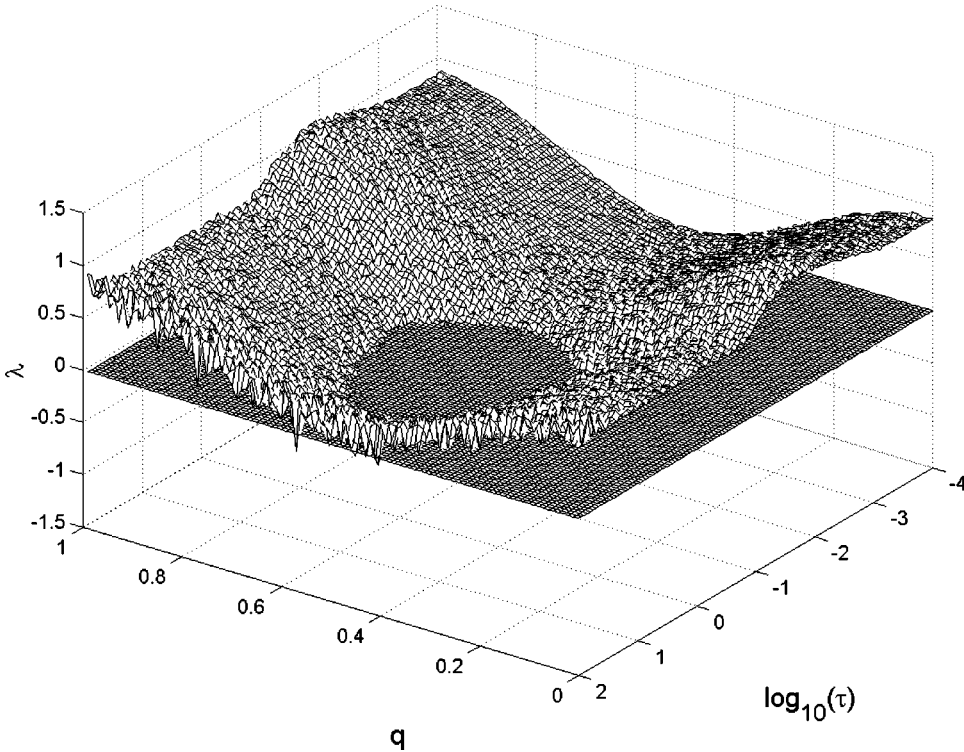


FIG. 3. Three-dimensional plot of the highest Lyapunov exponent λ as a function of time correlation $\log_{10}\tau$ and the reduced wave number $q = k/N$. The function $\lambda(q, \tau)$ crosses from positive (nonsynchronized state) to negative (synchronized state) for some critical values τ_c and q_c . Parameter values: $\sigma = 3$ and $D = 0.5$. Global noise was considered.

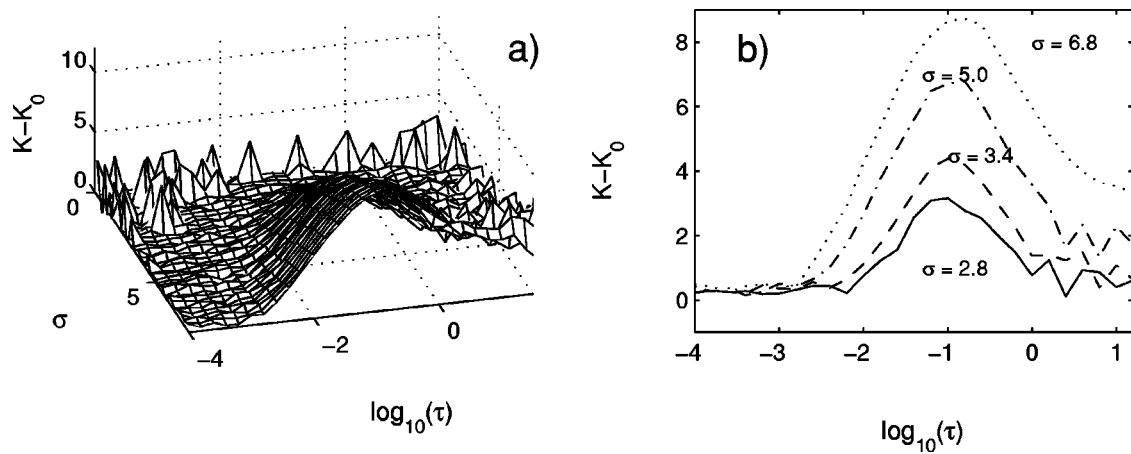


FIG. 4. (a) Three-dimensional plot of $K - K_0$ as a function of noise dispersion σ and time correlation τ and (b) sections of this plot for constant values of σ . Uncorrelated noise and periodic boundary conditions were considered. Parameter values: $N = 20$ and $D = 2.0$.

ment towards positive values, then deteriorating the chaotic synchronization between cells. This effect is more clearly shown in the profiles shown in Fig. 6(b) for constant values of R . Finally, Fig. 6(c) shows the nonmonotonic behavior of $K - K_0$ as a function of R for $\log_{10}\tau = -4$, when the white Gaussian limit is recovered. The dependence of τ_R and the maximum value of $K = K_{\max}$ with the bifurcation parameter R is shown in Fig. 7. The inset shows the calculated values of the mean oscillation period T for a single Lorenz cell calculated after a linear stability analysis was performed. In both cases, τ_R and T decrease with increasing values of R , while K_{\max} increases with R .

IV. DISCUSSION

Clearly, two effects have been described; (i) a locking between the characteristic frequency of the oscillator and the time correlation of the noise that is shown as a maximum for the function $K(\tau)$ for $\tau = \tau_R$, and (ii) an improvement or a poor synchronization between cells that depends on the coupling and noise strength, as well as on the proximity to the bifurcation point R_{cr} .

A. Resonant colored noise

The time-correlated Gaussian noise periodically modulates the attractor dynamics. A resonance effect between the chaotic attractor time scale and the noise correlation time τ should be expected, since the power spectrum of the noise cannot be considered to be flat within the frequency range of interest, τ^{-1} . The dependence of K on the time scale of the attractor, and the fact that the values of τ_R are within the main oscillation periods of the attractor, reinforce this point.

TABLE I. Critical values of q_c , N_c , and τ_c for which $\lambda(q, \tau)$ becomes negative. For $N_c \geq 4$, there is no value of τ_c for which λ is negative.

q_c	$N_c(k=1)$	τ_c (t.u.)
0.50	2	0.045
0.33	3	0.158
0.25	4	∞

To clarify this resonance effect, the noise term in the evolution equation for y of the Lorenz system, Eq. (1), has been modified in the following way:

$$\dot{y}_j = R(t) x_j - y_j - x_j z_j + D(y_{j+1} + y_{j-1} - 2y_j), \quad (5)$$

$$R(t) = R + \bar{\sigma} \cos \left[\frac{2\pi t}{\tau'} + \phi_j \right], \quad (6)$$

where the values of the amplitude $\bar{\sigma}$ and period τ' of the periodic forcing are equivalent to the noise dispersion σ and time correlation τ in Eq. (3). ϕ_j is an initial random phase which is different for each cell in the array, or equal for all cells depending on whether local or global forcings are considered.

Figures 8(a) and 8(b) show the dependence of $K - K_0$ with the forcing period τ' for the modified Lorenz model, Eqs. (5) and (6), for two different values of D . As well as for the time-correlated noise forcing, in this case K also shows a

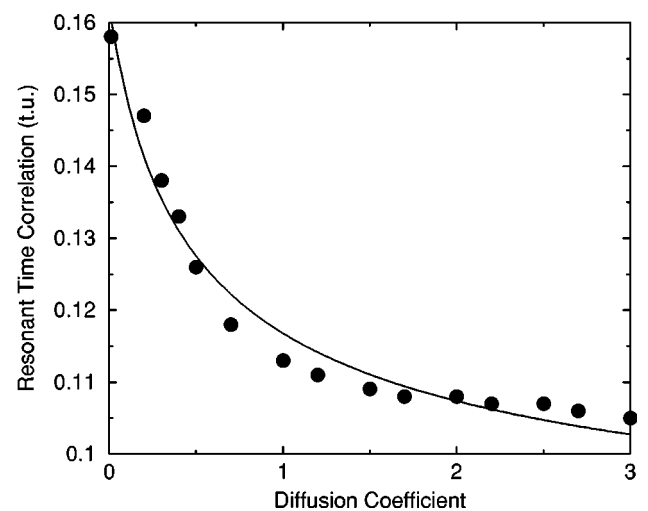


FIG. 5. Dependence of the resonant time correlation τ_R as a function of the coupling diffusion coefficient D for constant noise dispersion. The line represents a nonlinear fitting of the obtained values of τ_R to the equation $a_0 + a_1 / \sqrt{a_2 + D}$. Uncorrelated noise and free ends were considered. Parameter values: $N = 4$ and $\sigma = 3$.

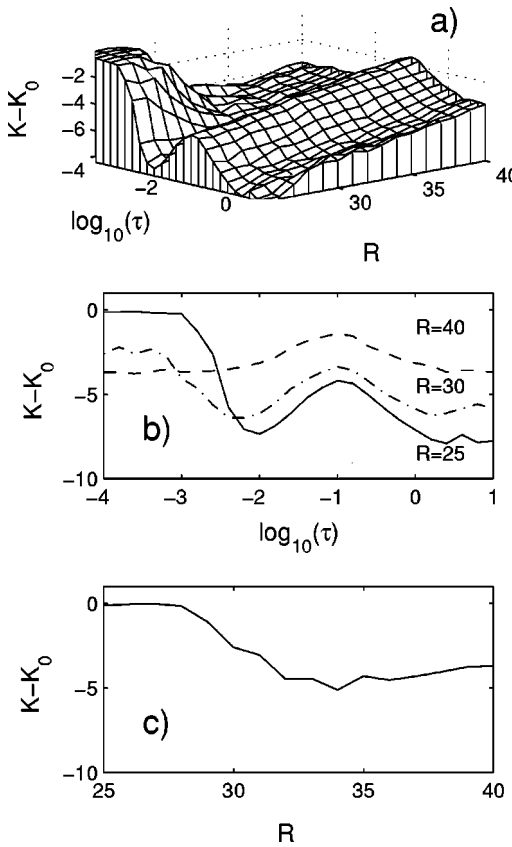


FIG. 6. (a) Three-dimensional plot of $K - K_0$ as a function of $\log_{10}\tau$ and the control parameter R in Eq. (1), (b) sections of this plot for three constant values of R , and (c) dependence of $K - K_0$ with R for the limit case of white Gaussian noise $\tau = 10^{-4}$. Parameter values: $N = 4$, $\sigma = 3$, and $D = 2$. Free ends were considered in the integration of Eq. (1).

maximum or a minimum value for some τ' depending on the coupling strength. Note that due to the single and well defined characteristic frequency of the forcing, the observed peaks are narrower than those obtained for the colored Gaussian noise, Fig. 1. Besides, the value of $\tau' = \tau'_R$ corresponding to the maximum and minimum of the function $(K - K_0)(\tau')$ in Figs. 8(a) and 8(b) is equal to the mean oscillation period of a single Lorenz cell for the selected set of parameters, $T = 0.61$ t.u. The measured values of τ'_R (or equivalent T) are greater than the corresponding values of τ_R , as was shown in Fig. 7 for different values of the bifurcation parameter R . Since by definition the time correlation τ

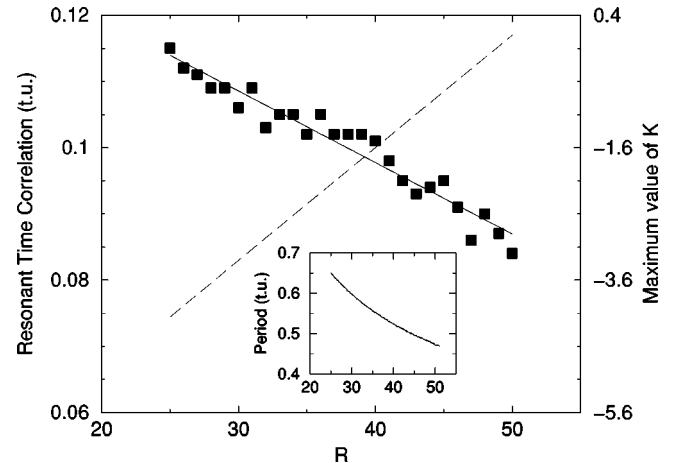


FIG. 7. Dependence of the resonant time correlation τ_R (left axis and black squares dots fitted to a straight line) and the maximum value of K (right axis and dashed line) as a function of the bifurcation parameter R . The inset shows the dependence of the mean oscillation period T of a single Lorenz equation as a function of R . Parameter values: $N = 4$, $\sigma = 3$, and $D = 2$. Free ends were considered in the integration of Eq. (1).

is the period of time that the values of $\xi(t)$ are correlated, then τ_R must be lower than T .

Then, although the resonance or locking between the natural frequency of the Lorenz oscillator and the time correlation of the colored Gaussian noise can be explained by this simple model depicted above, the enhancement or worsening of the chaotic synchronization implies a different mechanism.

B. Enhancement and worsening of the chaotic synchronization

Increasing the coupling strength between cells leads to an improvement of the chaotic synchronization since cluster formation (set of synchronized cells within the array) is favored. For a small number of cells, this effect is most notable as the number of possible different clusters diminishes as well, and then K tends to be smaller than K_0 . In Figs. 6 and 7, we showed that this behavior can be reversed as R increases. The maximum value of $K - K_0$ was also found to increase with R , finally leading to a poor synchronization (for $R > 49.5$, $K - K_0 > 0$ at least within the neighborhood of τ_R in Fig. 7). This phenomenon can be explained in terms of an *on-off intermittency* effect. Since in Eq. (1) the bifurcation parameter R is modulated by $\xi(t)$, the stationary probability

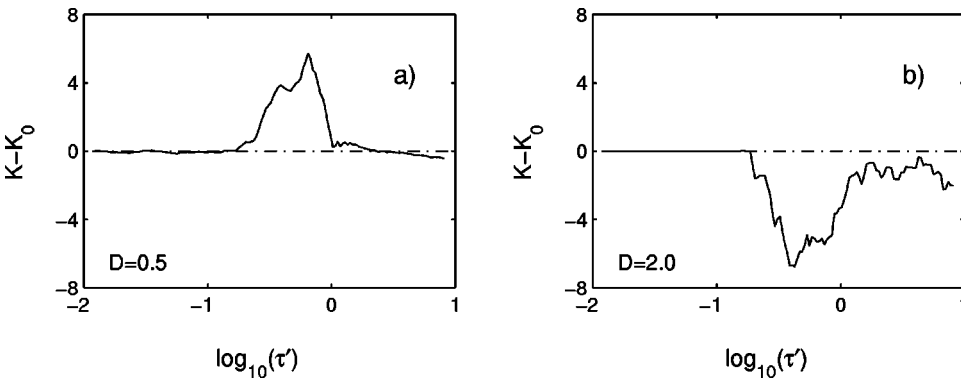


FIG. 8. Dependence of K with the forcing period τ' for the modified Lorenz model, Eqs. (5) and (6), for two different values of the diffusion coefficient; (a) $D = 0.5$ and (b) $D = 2.0$. Parameter values: $N = 4$ and $\bar{\sigma} = 3$. Free ends were considered and $\phi_i \neq \phi_j \quad \forall i, j = 1, \dots, N$.

to obtain values of $R(t) = R + \xi(t)$ smaller than R_{cr} where the attractor is not chaotic is given by [41]

$$\mathcal{P}(R(t) \leq R_{\text{cr}}) = \frac{1}{\sigma\sqrt{2\pi}} \int_{-\infty}^{R_{\text{cr}}} \exp\left(-\frac{(R' - R)^2}{2\sigma^2}\right) dR', \quad (7)$$

where clearly \mathcal{P} diminishes with increasing R .

Synchronization between cells is improved when the trajectories of each system become close to each other. This dynamical behavior occurs for $R(t) < R_{\text{cr}}$; the trajectories of the attractor tend to one of the two stable fixed points of the Lorenz system, and the distance between trajectories becomes smaller as t increases ($K \rightarrow 0$). In other words, the trajectories corresponding to the attractors of each cell in the array tend to be close to each other with a probability which is given by Eq. (7); i.e., the probability to have small values of the distance $\|\vec{u}_j^t - \vec{u}_{j-1}^t\|$ in Eq. (4) decreases with R . Then, the overall behavior of the function $K(\tau)$ should increase with R as was shown for K_{max} in Fig. 7. Of course, this behavior can be modified by increasing the value of σ , since then the decreasing rate of \mathcal{P} with R diminishes which in fact leads to a smaller increasing rate of K_{max} with R . Then, by controlling the values of σ and R it is possible to induce an improvement of the synchronization between cells in the array.

V. CONCLUSIONS

Synchronization of linearly coupled chaotic cells has been shown to be enhanced or worsened by multiplicative colored Gaussian noise. This phenomenon has been explained in terms of an on-off intermittency effect that occurs when the modulated bifurcation parameter $R(t) = R + \xi(t)$ crosses the bifurcation point at $R = R_{\text{cr}}$ that determines the stability of the Lorenz system. Optimum values of the noise and coupling strength have been obtained for enhanced array synchronization, and the effect of increasing number of cells in the array was also discussed. The effect of local and uncorrelated noises and the boundary conditions for solving Eq. (1) have also been investigated.

A locking between the time correlation τ and the time scale of the attractor has been observed. Here the noise correlation time competes with the time scale of the chaotic attractor to determine the realization and magnitude of the resonance phenomenon. This resonance cannot take place if the oscillators are not coupled.

These two phenomena depend on the way cells are coupled within the array as well as on the way the noise enters in the differential equations. By adding noise to a suitable bifurcation parameter, it is possible for a given value of the noise strength to visit regions of the phase space where the attractor is no longer chaotic, which in fact improves synchronization.

On the other hand, the issue of the dependence of our results on the characteristic time scale of the chaotic attractor deserves further comments. Those chaotic systems with longer time scales clearly need higher correlation times in order to achieve a resonance effect like the one described in

this paper. Nevertheless, as τ is increased, for a constant value of σ , the *effective* amplitude of the noise $A = \tau\sigma^2$ increases [see Eq. (3)], which in fact suppresses the resonance effect as the attractor turns out to be completely contaminated by noise. This is the case for other systems such as the Rossler model or the Hindmarsh-Rose neuronal attractor, among others.

Finally, one might speculate that the different behavior observed for weak and strong coupling among cells when the system is parametrically perturbed with time-correlated noise of low intensity could help in the laboratory, for example, to get an idea of the coupling and synchronization strength in neural networks involved in hippocampal epilepsy [46].

ACKNOWLEDGMENTS

We want to thank I.P. Mariño and I. Sendina-Nadal for fruitful discussions. This work was supported by DGES and Xunta de Galicia under Research Grants No. PB97-0540 and No. XUGA-20602B97, respectively.

APPENDIX: TRANSVERSE LYAPUNOV SPECTRUM

The effect of a colored noise on the chaotic synchronization of a ring consisting of chaotic Lorenz cells can be characterized by performing a linear stability analysis of the small deviations around the synchronized state [47]. Thus, if one considers a ring with N oscillators of dimension m the linear analysis of small perturbations will yield

$$\dot{\delta\mathbf{x}} = \mathbf{H} \delta\mathbf{x} \quad (A1)$$

for the differences between the variables of contiguous oscillators $\delta\mathbf{x}$, and where the Jacobian matrix \mathbf{H} of dimension $(Nm) \times (Nm)$ has N blocks of dimension $m \times m$, that have the same form as the linearized matrix for a single cell [48], and a number of off-block-diagonal terms arising from coupling. The most convenient form of analyzing such a setting is through the use of the discrete Fourier transform, due to the circulant structure of matrix \mathbf{H} [47,48]. What one obtains is that the original problem (A1) becomes uncoupled in terms of the Fourier transform η of the differences $\delta\mathbf{x}$ as follows:

$$\dot{\eta}^{(k)} = \mathbf{C}^{(k)} \eta^{(k)}, \quad (A2)$$

where \mathbf{C} is the Fourier transform of \mathbf{H} , $\eta^{(k)} = (1/N) \sum_{j=0}^{N-1} \delta\mathbf{x}_j e^{2\pi i j k / N}$ is the Fourier transform of $\delta\mathbf{x}$, and the $\mathbf{C}^{(k)}$ matrices take the form

$$\mathbf{C}^{(k)} = \begin{pmatrix} -\alpha & \alpha & 0 \\ R + \xi(t) - z & -1 + 2D(c_k - 1) & -x \\ y & x & -b \end{pmatrix}, \quad (A3)$$

with $c_k = \cos(2\pi k / N)$ and $k = 0, \dots, (N-1)$ the Fourier modes. Here, global or space-correlated noise $\xi(t)$ has been used in the calculations in order to have a circulant structure for the matrix \mathbf{H} in Eq. (A1).

The $k=0$ Fourier mode represents the uniform chaotic synchronized state of the ring, and the stability of this state can be characterized by analyzing the transverse spectrum, corresponding to Fourier modes with $k \neq 0$. As the system of Eqs. (1) is nonlinear, the $\mathbf{C}^{(k)}$ matrices have nonconstant, chaotically varying, coefficients. Thus, the stability is more conveniently analyzed through the corresponding Lyapunov exponents calculated from the $\mathbf{C}^{(k)}$ matrices (A3), yielding the transverse Lyapunov spectrum (TLS) [47]. The uniform mode $k=0$ will be stable whenever this spectrum is negative. An instability will arise in the moment in which some transverse Lyapunov exponent becomes positive. Instead of determining the transverse Lyapunov exponent for each couple (k, N) , a more practical procedure is to define the reduced wave number $q=k/N$ as a continuous variable in the range $[0, 1]$. The highest transverse Lyapunov exponent $\lambda(q)$

as a function of q may allow one to characterize the stability of the uniform synchronized state in a convenient way. An interesting remark is that $\lambda(q)$ should be symmetric with respect to the line $q=1/2$ since for a given N , $\mathbf{C}^{(k)}$ and $\mathbf{C}^{(N-k)}$ are the same matrices ($c_k = c_{N-k}$), implying the same property for their spectra of eigenvalues.

The function $\lambda(q)$ is obtained by using the procedure of Wolf *et al.* [49]. The transverse Lyapunov exponents are calculated for each wave number q from the $\mathbf{C}^{(k)}$ matrices (A3), where the nonconstant coefficients are obtained from the integration of Eq. (1) without diffusive coupling. Besides, the colored noise $\xi(t)$ in Eqs. (1) and (A3) is the same as global noise is being considered. Another important point to notice is that as $c_0=1$, the Lyapunov exponents corresponding to the uniform mode $k=q=0$ are identical to those of the isolated (uncoupled) chaotic system forced by the noise $\xi(t)$.

[1] E. Ott, C. Grebogi, and J.A. Yorke, Phys. Rev. Lett. **64**, 1196 (1990).

[2] T. Shinbrot, C. Grebogi, E. Ott, and J.A. Yorke, Nature (London) **363**, 411 (1993).

[3] G. Mayer-Kress and H. Haken, J. Stat. Phys. **26**, 149 (1981).

[4] I.I. Fedchenia, R. Mannella, P.V.E. McClintock, N.D. Stein, and N.G. Stocks, Phys. Rev. A **46**, 1769 (1992).

[5] P. Jung, Phys. Rep. **234**, 175 (1993).

[6] K. Wiesenfeld and F. Moss, Nature (London) **373**, 33 (1995).

[7] L. Gammaiton, P. Hänggi, P. Jung, and F. Marchesoni, Rev. Mod. Phys. **70**, 223 (1998).

[8] D.G. Luchinsky, P.V.E. McClintock, and D.I. Dykman, Rep. Prog. Phys. **61**, 889 (1998).

[9] B. McNamara, K. Wiesenfeld, and R. Roy, Phys. Rev. Lett. **60**, 2626 (1988).

[10] A. Simon and A. Libchaber, Phys. Rev. Lett. **68**, 3375 (1992).

[11] J. Stat. Phys. **70**, 1 (1993), edited by F. Moss, A. Bulsara, and M.F. Shlesinger.

[12] B. McNamara and K. Wiesenfeld, Phys. Rev. A **39**, 4854 (1989).

[13] V.S. Anishchenko, M.A. Safonova, and L.O. Chua, Int. J. Bifurcation Chaos Appl. Sci. Eng. **2**, 397 (1992); **4**, 441 (1994).

[14] V.M. Makeyev, Biophysics **38**, 189 (1993).

[15] M. Riani and E. Simonotto, Nuovo Cimento D **17**, 903 (1995).

[16] X. Pei, J. Wilkens, and F. Moss, J. Neurophysiol. **76**, 3002 (1996).

[17] M.E. Inchiosa and A.R. Bulsara, Phys. Rev. E **52**, 327 (1995).

[18] Y. Braiman, W.L. Ditto, K. Wiesenfeld, and M.L. Spano, Phys. Lett. A **206**, 54 (1995).

[19] Y. Braiman, J.F. Lindner, and W.L. Ditto, Nature (London) **378**, 465 (1995).

[20] P.C. Gailey, A. Neiman, J.J. Collins, and F. Moss, Phys. Rev. Lett. **79**, 4701 (1997).

[21] J.F. Lindner, B.K. Meadows, W.L. Ditto, M.E. Inchiosa, and A.R. Bulsara, Phys. Rev. Lett. **75**, 3 (1995); Phys. Rev. E **53**, 2081 (1996).

[22] A. Garfinkel, M.L. Spano, W.L. Ditto, and J.N. Weiss, Science **257**, 1230 (1992).

[23] S.J. Schiff, K. Jerger, D.H. Duong, T. Chang, M.L. Spano, and W.L. Ditto, Nature (London) **370**, 615 (1994).

[24] W.J. Freeman, H.J. Chang, B.C. Burke, P.A. Rose, and J. Bandler, IEEE Trans. Circuits Syst., I: Fundam. Theory Appl. **44**, 989 (1997).

[25] A. Maritan and J.R. Banavar, Phys. Rev. Lett. **72**, 1451 (1994).

[26] A.S. Pikovsky, Phys. Rev. Lett. **73**, 2931 (1994).

[27] A. Maritan and J.R. Banavar, Phys. Rev. Lett. **73**, 2932 (1994).

[28] H. Herzel and J. Freund, Phys. Rev. E **52**, 3238 (1995).

[29] G. Malescio, Phys. Rev. E **53**, 6551 (1996).

[30] P.M. Gade and C. Basu, Phys. Lett. A **217**, 21 (1996).

[31] L. Longa, E.M.F. Curado, and F.A. Oliveira, Phys. Rev. E **54**, R2201 (1996).

[32] E. Sánchez, M.A. Matías, and V. Pérez-Muñoz, Phys. Rev. E **56**, 4068 (1997); IEEE Trans. Circuits Syst. I: Fundam. Theory Appl. **46**, 495 (1999).

[33] P. Hänggi, P. Jung, C. Zerbe, and F. Moss, J. Stat. Phys. **70**, 25 (1993).

[34] Z. Gingl, L.B. Kiss, and F. Moss, Europhys. Lett. **29**, 191 (1995).

[35] S. Zhu, W. Yu, and R. Roy, Phys. Rev. A **34**, 4333 (1986).

[36] P. Hänggi, F. Marchesoni, and P. Grigolini, Z. Phys. B **56**, 33 (1984).

[37] J.L. Cabrera, J. Gorroño, and F.J. de la Rubia, Phys. Rev. Lett. **82**, 2816 (1999); J.L. Cabrera and F.J. de la Rubia, Europhys. Lett. **39**, 123 (1997).

[38] A.V. Barzykin, K. Seki, and F. Shibata, Phys. Rev. E **57**, 6555 (1998).

[39] E.N. Lorenz, J. Atmos. Sci. **20**, 130 (1963).

[40] C. Sparrow, *The Lorenz Equations: Bifurcations, Chaos and Strange Attractors* (Springer, New York, 1982), Vol. 41.

[41] J.M. Sancho, M. San Miguel, S.L. Katz, and J.D. Gunta, Phys. Rev. A **26**, 1589 (1982).

[42] V. Pérez-Muñoz and M.N. Lorenzo, Int. J. Bifurcation Chaos Appl. Sci. Eng. (to be published).

[43] R.F. Fox, I.R. Gatland, R. Roy, and G. Vemuri, Phys. Rev. A **38**, 5938 (1988).

[44] G. Benettin, L. Galgani, and J.M. Strelcyn, Phys. Rev. A **14**, 2338 (1976).

[45] M.A. Matías and J. Güémez, Phys. Rev. Lett. **72**, 1455 (1994).

[46] M.S. Jensen and Y. Yaari, J. Neurophysiol. **77**, 1224 (1997).

- [47] J.F. Heagy, T.L. Carroll, and L.M. Pecora, *Phys. Rev. E* **50**, 1874 (1994).
- [48] I.P. Mariño, V. Pérez-Muñuzuri, and M.A. Matías, *Int. J. Bifurcation Chaos Appl. Sci. Eng.* **8**, 1733 (1998); M.A. Matías, J. Güémez, V. Pérez-Muñuzuri, I.P. Mariño, M.N. Lorenzo, and V. Pérez-Villar, *Europhys. Lett.* **37**, 379 (1997).
- [49] A. Wolf, J.B. Swift, H.L. Swinney, and J.A. Vastano, *Physica D* **16**, 285 (1985).